Hyper-viscoelastic stress-softening modeling of pig perineal skin

Sarah Iaquinta, Grégory Chagnon, Anne-Sophie Caro

Hyper-viscoelastic stress-softening modeling of pig perineal skin

Sarah Iaquinta*
LMGC, IMT Mines Ales, Univ Montpellier, CNRS, Ales, France
Grégory Chagnon
Univ. Grenoble Alpes, CNRS, UMR 5525, VetAgro Sup, Grenoble INP, TIMC, Grenoble, France
Anne-Sophie Caro
LMGC, IMT Mines Ales, Univ Montpellier, CNRS, Ales, France

***Corresponding author.** sarah.iaquinta@mines-ales.fr

Keywords: perineal skin; hyperviscoelasticity; Mullins effect; relaxation.

1. Introduction

The pelvic floor, crucial for supporting pelvic organs and genitals, is prone to health issues commonly known as Pelvic Floor Dysfunctions (PFDs). The prevalence of at least one form of PFD (pelvic pain, pelvic organ prolapses, urinary or anal incontinence, dyspareunia) has been reported to be as high as 32% among females worldwide. Various factors such as older age, menopause, obesity, connective tissue disorders, or physical activity are significant contributors (Tim et al. 2021). However, the occurrence of PFDs is mainly due to traumatic events. Indeed, perineal tears, taking place in 90% of vaginal deliveries, have been identified to be a high-risk factor of PFDs (Jansson et al. 2020). Even though their effectiveness is not universally agreed upon within the medical community, some devices exist, leveraging the cyclic softening (Mullin's effect) observed in such soft tissues to delay the tears observed during childbirth. The preparation consists in using a probe (for example EPI-NO®) performing vaginal cyclic inflations. The objective of this publication is to characterize and model the pig perineal skin cyclic softening decoupling viscohyperelasticity and Mullins effect. Data from pure shear tests on pigs' perineal skin are used in conjunction with a 3D hyperviscoelastic model inspired of Rebouah et al., 2017 to propose a set of parameters that is suitable to describe loading, relaxation and unloading stages.

2. Methods

2.1 Materials

Skin tissues were extracted after dissection from porcine perinea supplied by the local slaughterhouse in Alès under the animal's welfare regulations (SEMAAC). Rectangular shapes were sampled from tissues of three pig perineum (Figure 1).

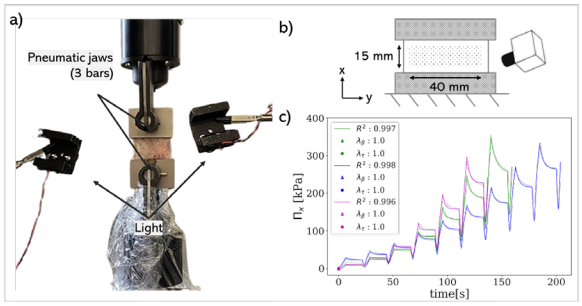

***Figure 1.** Device, sample geometry and pure shear stress (first Piola Kirchhoff) versus elongation*

2.2 Experiments

Instrumented pure-shear tests were conducted under a constant strain speed of $0.03s^{-1}$. The test consisted in applying cycles every 10% of elongation, each cycle being composed of traction, relaxation and unloading phases. Digital Image Correlation (DIC) enabled the evaluation of the in-plane strain.

2.3 Modeling

The Cauchy stress tensor is expressed as:

$$\bar{\bar{\sigma}}(t) = -p(t)\bar{\bar{I}} + \bar{\bar{\sigma}}_H(t) + \bar{\bar{F}}\bar{\bar{Q}}(t)\bar{\bar{F}}^T$$

where p is the pressure that ensure the incompressibility condition, $\bar{\bar{\sigma}}_H$ stands for the contribution of hyperelasticity (truncation of Rivlin modeling (Horgan & Smayda 2012)) and $\bar{\bar{Q}}(t)$ represents the contribution of the viscosity (Maxwell modeling):

$$\bar{\bar{\sigma}}_H(t) = 2\mathcal{F}(t)\frac{\partial W_H(t)}{\partial \bar{\bar{B}}(t)}\bar{\bar{B}}(t),$$

$$W_H(t) = c_{10}(I_1 - 3) + c_{01}(I_2 - 3) + c_{11}(I_1 - 3)(I_2 - 3),$$

$$\bar{\bar{\sigma}}_H(t) = \dot{\bar{\bar{Q}}}(t)\bar{\bar{B}}(t), \tau\dot{\bar{\bar{Q}}}(t) + \bar{\bar{Q}}(t) = \tau\beta\dot{\bar{\bar{S}}}_H(t),$$

$$\text{with } \bar{\bar{S}}_H(t) = \bar{\bar{F}}^{-1}\frac{\partial W_H(t)}{\partial \bar{\bar{B}}(t)}\bar{\bar{F}}^{-T},$$

where $\mathcal{F} = 1 - \eta\left(\frac{I_{1\,max} - I_1}{I_{1\,max} - 3}\right)^{\alpha}$, $\bar{\bar{B}}$ is the Cauchy Green tensor, $\bar{\bar{F}}$ is the deformation gradient, W_H is the density of energy, I_1, I_2 are the first and second strain invariants depending on stretches ratio, and c_{10}, c_{01}, c_{11}, τ, β, η, α are the material parameters.

In the case of pure in plane shear test for which transverse stretch ratio are assumed to be equal to 1 the axial Cauchy stress component is reduced to:

$$\sigma_{xx}(t) = 2\mathcal{F}(t)\left(\frac{\partial W_H(t)}{\partial B_x(t)} - \frac{\partial W_H(t)}{\partial B_z(t)}\right)\left(\lambda_x^2(t) - \lambda_x^{-2}(t)\right) + Q_x(t)\lambda_x^2(t)$$

3. Results and discussion

DIC enabled the validation of pure shear stress assumption. As observed in Figure 1, relaxation behavior highly depends on elongation. It is therefore expected that relaxations time and associated weight evolve during stretching. Surgeman et al., 2020

confirm these assumptions on blood clots. Indeed, material parameters τ (relaxation time) and β (weight parameter) are expected to be at first constant and then linearly evolve (to minimize the number of material parameters to be fitted) during stretching:

$\tau = a_\tau \lambda_x + b_\tau, \lambda_x \geq \lambda_\tau$ and $\tau = \tau_0$ otherwise ;

$\beta = a_\beta \lambda_x + b_\beta, \lambda_x \geq \lambda_\beta$ and $\beta = \beta_0$ otherwise,

where $a_\tau, a_\beta, b_\tau, b_\beta, \tau_0, \beta_0, \lambda_\tau, \lambda_\beta$ are material parameters. b_τ and b_β were evaluated at every load cycle in terms of the other parameters.

A set of parameters that produced the best fit of the experimentally measured stress by the first Piola Kirchhoff stress Π (minimization of $|R^2 - 1|$ using the Scipy L-BFGS-B bound constrained quasi-Newton optimization algorithm (Byrd et al. 1995)) is proposed in Table 1. Experimental and numerical results are presented in Figure 1. The fitted response reproduced well the loading, relaxation and unloading phases.

***Table 1**. material parameters (CoV = std/mean).*

a - hyperelasticity and Mullins effect

Sample	c_{10}, c_{01}, c_{11} (kPa)	η (-)	α (-)
1	0.25, 0.25, 25.5	0.28	0.28
2	15.3, 0, 12.3	0.71	0.53
3	0, 0, 31.0	0.32	0.31
mean	5.18, 0.08, 22.9	0.44	0.37
std	8.76, 0.14, 9.61	0.24	0.14
CoV	1.69, 1.73, 0.42	0.54	0.37

b – relaxation

Sample	a_τ(-)	a_β (s^{-1})	τ_0(s)	β_0(-)	λ_τ(-)	λ_β(-)
1	9.8	10	0.29	2.44	1	1
2	0.9	4.9	2.41	4.78	1	1
3	7.7	6.48	0.15	3.61	1	1
mean	6.13	10.5	0.95	3.61	1	1
std	4.65	4.22	1.27	1.17	0	0
CoV	0.76	0.40	1.33	0.32	0	0

The best fit ($R^2 > 0.99$) for the three samples was obtained with $\lambda_\tau = \lambda_\beta = 1$, demonstrating that (i) the viscoelastic response of the material is altered by the level of strain, (ii) the relaxation time τ and the weight of viscoelasticity compared to hyperelasticity, identified by the parameter β, evolve from the beginning of the test and not after a shift strain. Furthermore, the values identified for the variation of β were of the same order of magnitude (CoV = 0.4 and 0.32 for a_β and β_0, respectively). It *was* also the case for the Mul*l*ins effect parameters (CoV = 0.54 and 0.35 for η and α, respectively). The hyperelastic parameters provided more variable results (CoV = 1.69 and 1.73 for c_{10} and c_{01}, respectively). These results suggest that the weight parameter β and the stress softening-related parameters η and α are less likely to be sensitive to the commonly encountered variability in biological specimens than the hyperelastic parameters (especially c_{10} and c_{01}). Still, this assumption needs to be verified with more samples and using different strain rates to verify that the results presented in this work also apply.

3. Conclusions

This work was a first step in the modeling of the sensitivity of the viscoelastic contribution to the strain level. A phenomenological validation of this result needs to be conducted via microstructural observation questioning the anisotropy induced by the stretching. The evolution of the contribution of viscoelasticity, associated with Mullins effect seems to be a promising effective, reliable, and reproducible way to track mechanical changes before it impacts macroscopically the stress level.

Acknowledgements [Style Acknow_SB]

The authors are thankful to Cristina Cavinato, Romain Léger and Jonathan Barés for the sample preparation, testing and post-processing.

This project was supported by the LabEx NUMEV (ANR-10-LABX-0020) within the I-Site MUSE (ANR-16-IDEX-0006).

Conflict of Interest Statement

The authors have no conflict of interest to declare.

References

Tim, S., Mazur-Bialy, A. I. (2021) The most common functional disorders and factors affecting female pelvic floor. *Life (Basel)*, 11(12), 1397-1415.

Jansson, M. H., Franzén, K., Hiyoshi, A. Tegerstedt, G., Dahlgren, H., Nilsson, K. (2020) Risk factors for perineal and vaginal tears in primiparous women - the prospective POPRACT-cohort study. *BMC Pregrancy Childbirth*, 20 (1), 749-763. doi: 10.1186/s12884-020-03447-0

Rebouah, M., Chagnon, G., Heuillet, P. (2017) Anisotropic viscoelastic models inlarge deformation for architectured membranes. *Mechanics of Time-Dependent Materials* 21 (176), 163-176.

Horgan, C. O., & Smayda, M. G. (2012). The importance of the second strain invariant in the constitutive modeling of elastomers and soft biomaterials. Mechanics of Materials, 51, 43-52.

Surgerman G., P., Parekh, S. H., Rausch, M. K. (2020) Nonlinear, dissipative phenomena in whole blood clot mechanics. Soft Matter, 16, 9908-9916. doi: 10.1039/d0sm01317j

Byrd, R. H., Lu P., Nocedal J. (1995) A Limited Memory Algorithm for Bound Constrained Optimization. *SIAM Journal on Scientific and Statistical Computing*, 16 (5), 1190-1208.

Received date:07/04/2024
Accepted date: 28/06/2024
Published date: XX/XX/2024
Volume: 1
Publication year: 2024